Revista Brasileira de Ciência do Solo

Division – Soil in Space and Time | Commission – Soil Genesis and Morphology

Chemical-Mineralogical Characterization of Magnetic Materials from Magnetic Soils of the Southern Espinhaço Mountain Chain and of the Upper Jequitinhonha Valley, State of Minas Gerais, Brazil

Alexandre Christófaro Silva[(1)*], Solange de Souza[(2)], José Domingos Fabris[(3)], Maurício Soares Barbosa[(4)], Uidemar Morais Barral[(4)] and Roberto Vial Costa[(4)]

[(1)] Universidade Federal dos Vales do Jequitinhonha e Mucuri, Departamento de Engenharia Florestal, Diamantina, Minas Gerais, Brasil.
[(2)] Universidade Federal dos Vales do Jequitinhonha e Mucuri, Instituto de Ciência e Tecnologia, Diamantina, Minas Gerais, Brasil.
[(3)] Universidade Federal dos Vales do Jequitinhonha e Mucuri, Departamento de Quimica, Diamantina, Minas Gerais, Brasil.
[(4)] Universidade Federal dos Vales do Jequitinhonha e Mucuri, Departamento de Agronomia, Programa de Pós-graduação em Produção Vegetal, Diamantina, Minas Gerais, Brasil.

*** Corresponding author:**
E-mail: alexandre.christo@ufvjm.edu.br

Received: May 30, 2016
Approved: September 23, 2016

How to cite: Silva AC, Souza S, Fabris JD, Barbosa MS, Barral UM, Costa RV. Chemical-mineralogical characterization of magnetic materials from magnetic soils of the southern Espinhaço Mountain Chain and of the Upper Jequitinhonha Valley, state of Minas Gerais, Brazil. Rev Bras Cienc Solo. 2017;41:e0160274.
https://doi.org/10.1590/18069657rbcs20160274

ABSTRACT: In the Southern Espinhaço Mountain Chain and in the Upper Jequitinhonha Valley, magnetic soils, in different pedogenetic stages, are found to be forming over intrusions of basic lithology. The essential chemical and mineralogical properties of samples from magnetic soil profiles from those two physiographic environments in the state of Minas Gerais, Brazil, are reported. Three of the pedons (Rhodic Kandiustox – RKox, Rhodic Haplustox – RHox, and Typic Argiustoll - TAoll) were identified as being indeed developed over basic rocks; the fourth *pedon* (Typic Haplustox - THox) is currently forming on an acidic rock. Particle size and routine chemical analyses were performed on samples from all horizons of the four selected soil profiles. For a deeper insight into the dominant mineralogy of each diagnostic soil horizon, the elemental contents, expressed in terms of the corresponding metal cation oxides, namely Fe_2O_3, Al_2O_3, and MnO_2, were obtained from digesting the whole soil samples with sulfuric acid. A similar chemical analytical procedure was performed for the residual solid extracts obtained from attacking the whole soil materials with mixtures of (i) dithionite - citrate - bicarbonate and (ii) oxalate - oxalic acid. The soil samples were also analyzed by Mössbauer spectroscopy at room temperature (~298 °K) in an attempt to better identify the main magnetic iron oxides. Maghemite (δFe_2O_3) was found in all samples and magnetite (Fe_3O_4) was identified only for the sample from the Typic Argiustoll. The pedogenetic loss of silica and consequent accumulation of iron and aluminum oxides along the profile are found to be somehow correlated to the weathering sequence in the soils forming on basic rocks: TAoll < RKox < RHox.

Keywords: iron oxides, X ray diffractometry, Mössbauer spectroscopy, scanning electron microscopy, energy dispersive spectroscopy.

INTRODUCTION

The Southern Espinhaço Mountain Chain (SdEM) occupies approximately 3.7 million ha in 53 municipalities of the state of Minas Gerais, Brazil. The topography is predominantly mountainous, where quartzite rocks predominate, associated with Entisols and gravelly and sandy soils. The rural population lives mainly in areas where there are Oxisols and dystroferric and magnetic (Santos et al., 2013) rocks, originating from basic rocks that have chemical and physical properties that permit their use for crops, both for family farms and for corporate use.

The Upper Jequitinhonha Valley (UJV) borders on the SdEM and covers approximately 2 million hectares (Portal da Cidadania, 2012). The UJV geomorphology is characterized by plateaus, flat or gently rolling areas, with average altitudes of around 900 m, which alternate with areas divided by the Jequitinhonha River and its affluents, dominated by ravine slopes and hills (Minas Gerais, 1983). The UJV rural population lives in dissected plateau areas, consisting mainly of family farms, in which basic rock soils, such as dystroferric and eutroferric Oxisols and Chernosols with high agricultural potential, originated. Dystroferric Oxisols originating from acidic rocks occur in the plateau region. These areas are commercially exploited by growing eucalyptus and coffee, and raising cattle under technological agricultural systems utilized by large and medium-sized companies.

Magnetic soils have a saturation magnetization of soil mass higher than 1 J T^{-1} kg^{-1} (Resende et al., 1986). They commonly have relatively high proportions of iron oxides with ferrimagnetic structures, such as maghemite (γFe_2O_3) and magnetite (Fe_3O_4), and are identified in the field by response of the soil mass to a magnetic field, involving immediate adhesion of mineral particles to a hand magnet. In the laboratory, they are identified by Mössbauer spectroscopy (Fabris et al., 1998).

Iron oxides, neoformed from the release of iron ions into the soil by weathering of primary (lithogenic) or secondary (pedogenic) minerals, are a group of minerals characterized as being indicators sensitive to environmental conditions and pedogenic processes (Schwertmann and Taylor, 1989). They are widely used as pedoenvironment indicators, and the study of their properties may reveal information regarding past events and current circumstances relevant to soil formation (Kämpf and Curi, 2000; Muggler et al., 2001; Inda Junior and Kämpf, 2003; Cunha et al., 2005; Figueiredo et al., 2006). The magnetic activity can be correlated with the availability of Cu, Mn, Zn, Mo, and Ni, which are essential for plant nutrition (Resende et al., 1988; Ferreira et al., 1994).

The contents of iron oxides from soils derived from basic and acidic rocks of the SdEM and UJV and their magnetic structural features are related to the source material (magmatic rocks), pedogenic processes (residual concentration of iron oxides after removal of Si and bases and oxidation of Fe^{2+} in magnetite and its transformation to maghemite) and the past and current environmental conditions (Kämpf and Curi, 2000).

The chemical and mineralogical properties essential to characterization of four materials sampled from magnetic soil profiles are described in this study. Three of these materials (Rhodic Kandiustox – RKox, Rhodic Haplustox – RHox, and Typic Argiustoll – TAoll) developed from basic and acidic rock (Typic Haplustox - THox) of the SdEM and UJV, which are both physiographic regions of the state of Minas Gerais, Brazil. The studies focus especially on the properties of the ferrimagnetic structures derived from iron oxides to identify the dominant pedogenetic processes and to determine the weathering sequence involving mineralogical changes in iron oxides in the transformation of rock to soil.

MATERIALS AND METHODS

Characterization of environments

Soil profiles of the SdEM and UJV were described, and soil samples were collected from all horizons. The geosystem denominated the SdEM corresponds to a massive set of undulated structural reliefs, broken and uneven in faulting, developed in or through conglomeratic quartzites, with lenticular interbedded formed by phyllites and schists of the Espinhaço Supergroup (Brasil, 1997). The quartzite rocks are cut through by basic igneous rocks, with magnetism. The events that occurred date from 902±2 million years ago (Almeida-Abreu and Renger, 2002).

In UVJ, based on lithologies of the Macaúbas Group, flattened areas called "Chapadas" meet with slopes below 10 % and medium altitudes around 900 m, separated by dissected valleys. The Planalto de Minas formation of the Macaúbas Group is mainly composed of green schist (metabasalts) that occur particularly in the area of the Planalto de Minas and Desembargador Otoni districts in the municipalities of Diamantina and Carbonita (Chula, 1998; Gradim et al., 2005).

The SdEM climate is predominantly mesothermal, Cwb in the Köppen classification system, with average annual rainfall between 1,250 and 1,550 mm and average annual temperature between 18 and 19 °C (Silva et al., 2005). According to Vilhena et al. (2010), the predominant climate of the UVJ is Aw, rainfall ranges from 600 to 1,200 mm, and the average annual temperature is between 21 and 24 °C.

The vegetation in the SdEM and UVJ is characteristic of the Cerrado (Brazilian tropical savanna) Biome. In the SdEM, there are the rupestre vegetation types (Silva et al., 2005); semideciduous forest fragments at the borders of the "Chapadas" can be found in UVJ (Bispo et al., 2011a).

Fieldwork

Four soil profiles were selected in the SdEM and UVJ that depended on the source material, location, and developmental stage. These profiles, situated at altitudes ranging from 731 to 1,236 m, were described morphologically according to Santos et al. (2005).They were sampled in order to conduct physical, chemical, and mineralogical analyses and classified according to the Brazilian System of Soil Classification, SiBCS (Santos et al., 2013) and Soil Taxonomy (Soil Survey Staff, 2010). The profiles were classified as *Nitossolo Vermelho Distroférrico típico – NVdf* (Rhodic Kandiustox - RKox) (P1 profile), well drained, coming from green schist located in the area with gently rolling relief, colonized by *Cerrado* vegetation, without agricultural use, located in the Planalto de Minas district, municipality of Diamantina (676976E 8045963S, 750 m - UVJ); *Latossolo Vermelho Distrófico típico - LVdf* (Typic Haplustox - THox) (P2 profile), very well drained, coming from Salinas schist, situated in a flat terrain area originally colonized by Cerrado vegetation and cultivated with eucalyptus, located in the municipality of Tourmaline (0722646E 8090180S, 894 m - UVJ); *Latossolo Vermelho Distróférrico típico - LVd* (Rhodic Haplustox - RHox) (P3 profile), very well drained, coming from gabbro, located in an area of rolling relief, colonized by vegetation of semi-deciduous forest and no agricultural use, located in the Pinheiro district, municipality of Diamantina (644289E 8000956S, 1052 m - SdEM); and *Chernossolo Argilúvico Órtico saprolítico – MTo* (Typic Argiustoll - TAoll) (P4 profile), well to moderately drained, located in an area of strongly rolling relief, coming from green schist, originally colonized by *Cerrado* vegetation and cultivated with coffee, located in the Retiro Community, municipality of Carbonite (0697715E 8075961S, 746m - UVJ). The essential information is shown in figure 1.

Laboratory work

Particle size was determined by the pipette method (Claessen, 1997), and routine chemical analyses were performed according to Claessen (1997) in all horizons of the four soil profiles.

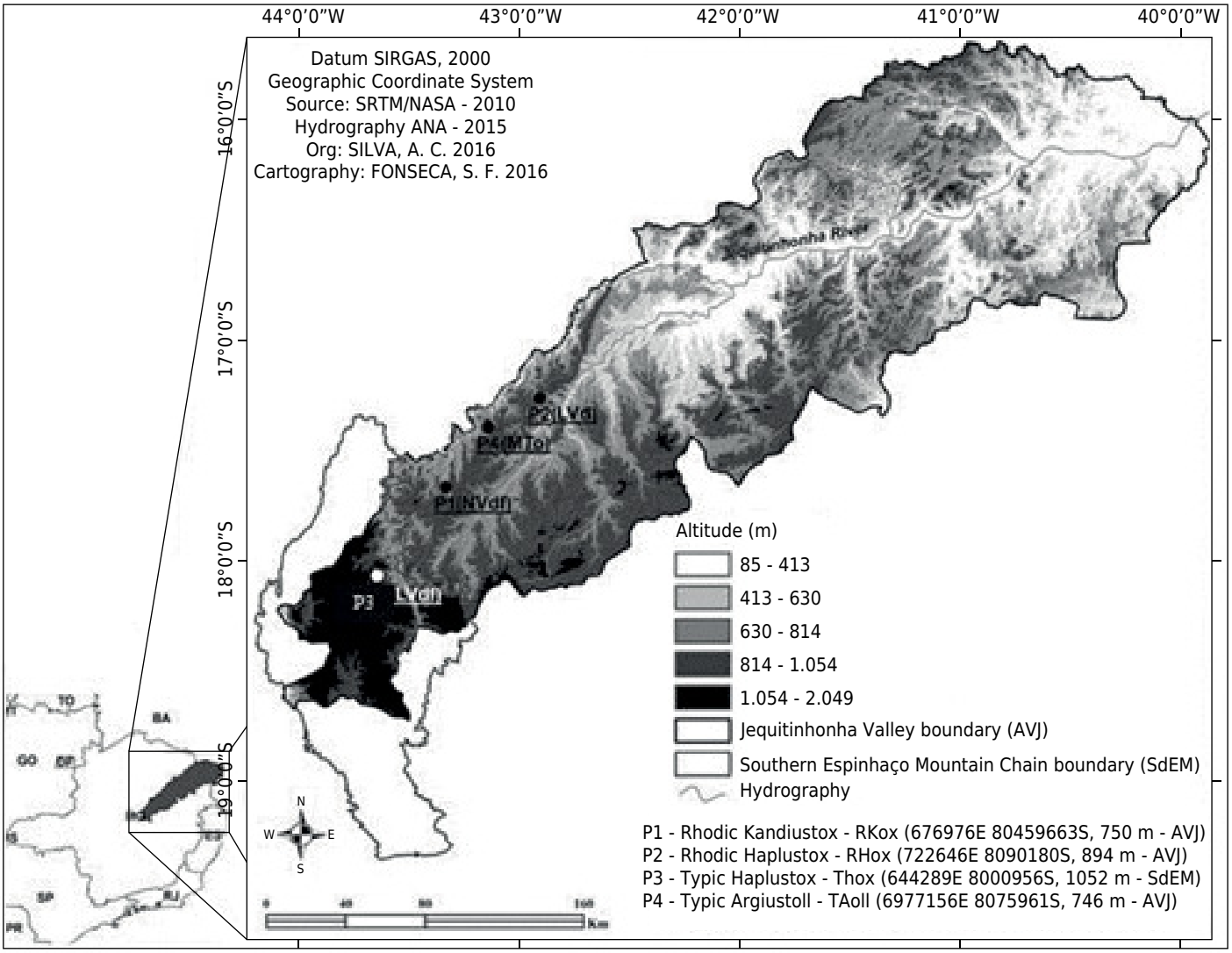

Figure 1. Geographical map identifying the sampling sites in the Southern Espinhaço Mountain Chain and Upper Jequitinhonha Valley.

Crystalline oxides and low crystallinity forms of Fe, Al, and Mn were dissolved in the soil samples from each diagnostic horizon. For dissolution of crystalline oxides, a 0.3 mol L^{-1} dithionite-citrate-bicarbonate (DCB) mixture in the proportion of 1:40 was heated in a water bath at 75 °C under constant agitation for 15 min and centrifuged at 2,500 rpm for 15 min (Mehra and Jackson, 1960; Claessen, 1997; Inda Junior and Kämpf, 2003). The Fe, Al, and Mn forms of low crystallinity were dissolved with 0.2 mol L^{-1} ammonium oxalate (AAO) at pH 3.0 in the ratio 1:40, shaken in the dark for 4 h, and subsequently centrifuged at 2,500 rpm for 15 min (McKeague and Day, 1966; Schwertmann and Taylor, 1977). Starting with the products solubilized by DCB and OAA, the contents of Fe, Al, and Mn were quantified by atomic absorption spectrophotometry.

The total contents of Fe, Al, Ti, Mn, and Si oxides were determined after treating the soil samples of each diagnostic horizon with an equal volume of H_2SO_4 (sulfuric acid attack), according to the method described by Claessen (1997). The oxide contents obtained by sulfuric acid attack were used to calculate the molecular ratios Ki = (%SiO_2 × 1.697)/% Al_2O_3; and Kr = (%SiO_2 × 1.697)/[(%Al_2O_3) + (%Fe_2O_3 × 0.64)].

X ray diffraction

The clay mineralogy fraction was determined by X ray (XRD) diffraction using a Shimadzu XRD-6000 diffractometer with a copper anode tube and coupled graphite crystal monochromator, scan speed of 2° 2θ min^{-1}, and scan range from 3° to 90° 2θ', with accelerating voltage and

current of 40 kV/20 mA. Preparation and treatment of samples for determining the composition of the free clay fractions were performed according to Jackson (1969). The samples of the iron-free clay fraction in paste form were saturated with K^+ (1 mol L^{-1} KCl) and Mg^{2+} (1 mol L^{-1} $MgCl_2$), according to the method proposed by Theisen and Harward (1962).

Iron oxide mineralogy was analyzed by pretreatment of the samples with 5 mol L^{-1} NaOH, according to the procedure described by Norrish and Taylor (1961), modified by Kämpf and Schwertmann (1982).The data obtained from the XRD were plotted, and the criteria used to interpret the XRD patterns and to identify the mineral constituents of the clay and sand fractions were based on the interplanar spacing and angular displacements of the reflection peaks for the samples treated by saturating cations (K^+ and Mg^{2+}) and heating effects (350 °C and 550 °C for the samples saturated with K^+) as recommended by Jackson (1969), Brown and Brindley (1980), and Moore and Reynolds (1989).

Mössbauer spectroscopy

For the sample diagnosis horizon of each soil, the hyperfine structure of ^{57}Fe relative to ferruginous minerals, particularly iron oxides, was analyzed by Mössbauer spectroscopy at room temperature (~ 298K). Mössbauer spectra of the samples were obtained in transmission mode with a variation in the Doppler velocity constant acceleration system of the ^{57}Co source in an Rh matrix (Fabris and Coey, 2002; Fabris et al., 2009).

All the spectra were recorded on a memory unit with 512 channels in MCS mode and Doppler speed in the approximate speed ranges between ±10 and ±12 mm s^{-1}, calibrated with a metallic Fe absorber (αFe sheet). Samples with an Fe ratio of ~10 mg cm^{-2}, diluted in a mixture with sugar, were placed in tablets in sample holders. The spectral data were numerically fitted with a Lorentzian function by the least squares method, using the WinNormos-for-Igor® computer program.

Scanning electron microscopy and dispersive energy spectroscopy

Characterization of the chemical composition (sand, silt, clay, and the magnetic fraction separated with a hand magnet) of samples of the diagnostic horizon of each soil was performed by energy dispersive spectroscopy (EDS). Micrographic images of the samples were obtained with the Hitachi Scanning Microscope operating at 5 and 15 kV.

RESULTS AND DISCUSSION

The clay fraction is prevalent in almost all soils (Table 1), and levels range from 290 to 790 g kg^{-1}. The lowest sand contents were found in the RHox, THox, and TAoll, whereas the highest silt contents were found in the TAoll (Table 1), which is common for this soil class (Troeh and Thompson, 2007). The low silt/clay ratio in Oxisols is related to its advanced stage of weathering (Resende et al., 2007). The intermediate and high levels of silt/clay ratios of the RKox and TAoll, respectively, reflect a lower weathering stage, especially in the TAoll (Resende et al., 2007). Ferreira et al. (2010) and Bispo et al. (2011a) also found low values for the silt/clay ratio of Oxisols for the UVJ, as well as Silva et al. (2005) for Oxisols for the SdEM.

The P values were very low in all the horizons of all the soils, except in the BA horizon of the TAoll (Table 2). According to Vahl (1999), P is fixed by oxides, oxy-hydroxides, and Fe and Al hydroxides, which prevent their release into the soil solution. Oxisols have high P adsorption power (Leal, 1971; Novais et al., 1991). The higher levels of P in the BA horizon of the TAoll may result from a slightly weathered profile, with pH around 6.0 (Table 2), that originated from green schist formed by mineral-rich P rock (Chaves and Vasconcelos, 2006).

Oxisols had low levels of Ca. The RKox and TAoll originating from green schist have the highest levels of Ca; the levels were very high in the TAoll, a less weathered soil (Table 2). Novais et al. (2007) indicate that Ca minerals are weathered slightly faster

Table 1. Particle fraction distribution in soils of the Southern Espinhaço Mountain Chain and Upper Jequitinhonha Valley

Horizon	Depth	Sand	Silt	Clay	Silt/clay ratio
	m	g kg^{-1}			
P1- *Nitossolo Vermelho Distroférrico típico - NVdf* (Rhodic Kandiustox - RKox)					
A	0.00-0.27	150	310	540	0.57
AB	0.27-0.57	130	310	560	0.55
Bn_1	0.57-0.94	110	360	520	0.69
Bn_2	0.94-1.30+	130	210	660	0.32
P2 - *Latossolo Vermelho Distróférrico típico - LVdf* (Rhodic Haplustox - RHox)					
A	0.00-0.26	230	270	500	0.54
AB	0.26-0.47	200	230	570	0.40
BA	0.47-0.80	190	220	590	0.37
BW	0.80-1.50+	180	280	540	0.52
P3 - *Latossolo Vermelho Distrófico típico - LVd* (Typic Haplustox - THox)					
A	0.00-0.23	100	170	730	0.23
AB	0.23-0.41	100	200	710	0.28
BA	0.41-0.74	90	160	750	0.21
Bw	0.74-2.0+	90	120	790	0.15
P4 - *Chernossolo Argilúvico Órtico saprolítico - MTo* (Typic Argiustoll - TAoll)					
A	0.00-0.19	200	480	330	1.45
BA	0.19-0.34	110	420	470	0.89
Bt	0.34-0.58	140	430	430	1.00
BC	0.58-0.74	140	570	290	1.96
CR	0.74-0.90+	200	490	310	1.58

Sand, silt, clay: pipette method.

than the average for minerals from the soil, and there is tendency for Ca content in the soil to gradually decline with weathering processes and leaching. This corroborates the results (TAoll >> RKox > THox ~ RHox). Good drainage of soils, especially the Oxisols, also contributes to greater Ca leaching (Troeh and Thompson, 2007).

Magnesium levels were also lower in the RHox and THox, intermediate in the RKox, and higher in the TAoll (Table 2), in accordance with the weathering sequence of the soils. The Mg content in the soil can be explained by several factors, including its relationship with ferromagnesian minerals, such as in the TAoll, derivatives, for example, of biotite (Troeh and Thompson, 2007). As for Ca, the very good drainage of the Oxisols also contributed to greater Mg leaching (Troeh and Thompson, 2007).

The sum of bases (SB), cation exchange capacity (CEC) and organic matter content decreased with depth in all the soils, except for the TAoll. In Oxisols, the T is greater on the surface because of the higher organic matter content (Table 2). The T of the TAoll is very high, and this can be related to the presence of 2:1 clay (Costa, 2014) and to its initial weathering stage.

Base saturation (V) ranged from 3 to 93 %. The TAoll had a very high V, reaching 93 %. The high levels of Ca and Mg and the low degree of weathering (silt/clay ratio greater than 1 - Table 1) contribute to a high V in the TAoll (Resende et al., 1988; Novais et al., 2007). The RKox of basic rock origin had a V between 37 and 66 %. The V is also influenced by the source material, with a tendency to be higher in soils derived from gabbro and green schist and lower in soils derived from acidic rock (Popp, 1998). Highly weathered Oxisols have saturation baselines lower than 43 % (Table 2). Ferreira et al. (2010) and Bispo et al. (2011a) obtained similar values in Oxisol toposequences of UVJ plateaus.

In very well drained Oxisols, Al saturation (m) was higher in the surface layers, which concentrate the organic matter of the profiles (Table 2) and confirm the results found by Inda Junior et al. (2007) and Resende et al. (1988).

The SiO_2 contents decrease and Al_2O_3 and Fe_2O_3 correspondingly increase in the following sequence of basic rock soil: TAoll > RKox > RHox (Table 3), and demonstrate the processes of desilicatization and ferralitization resulting from the intensification of weathering.

All soils showed Fe_2O_3 contents above 10 %, which were higher in ferric soils (RKox and RHox) and lower in the soil originating from acidic rock (THox) (Table 3). The presence of iron compounds in the soil varies with the source material, degree of weathering, and

Table 2. Chemical properties of soils of the Southern Espinhaço Mountain Chain and Upper Jequitinhonha Valley

Horizon	OM	pH(H_2O)	P	K	Ca^{2+}	Mg^{2+}	Al^{3+}	H+Al	SB	t	CEC	m	V
	dag kg^{-1}		mg kg^{-1}		$cmol_c$ kg^{-1}							%	
P1- *Nitossolo Vermelho Distroférrico típico - NVdf* (Rhodic Kandiustox - RKox)													
A	1.20	5.30	1.90	23.46	4.30	2.50	0.30	4.90	6.86	7.16	11.76	4.19	58.33
AB	1.30	5.50	2.10	15.64	2.70	2.40	0.60	2.10	5.14	5.74	7.24	10.45	70.99
Bn1	1.10	5.60	0.30	23.33	2.70	1.90	1.10	4.70	5.12	6.22	9.82	17.68	52.14
Bn2	0.70	5.80	0.30	7.82	2.70	1.90	0.60	5.20	4.62	5.22	9.82	11.49	47.05
P2 - *Latossolo Vermelho Distroférrico típico - LVdf* (Rhodic Haplustox - RHox)													
A	1.10	5.10	1.88	27.37	0.18	0.10	0.93	5.57	0.35	1.28	5.92	72.66	5.91
AB	0.50	5.30	1.25	7.82	0.08	0.04	0.36	3.84	0.14	0.50	3.98	72.00	3.52
BA	0.10	5.40	1.96	3.91	0.12	0.08	0.09	2.61	0.21	0.30	2.82	30.00	7.45
Bw	0.80	5.50	3.22	3.91	0.09	0.03	0.03	1.87	0.13	0.16	2.00	18.75	6.50
P3 - *Latossolo Vermelho Distrófico típico - LVdf* (Typic Haplustox - THox)													
A	3.70	4.50	1.00	19.55	1.80	1.30	2.00	9.40	3.15	5.15	12.55	38.83	25.10
AB	1.30	5.10	0.10	3.91	1.60	1.20	1.30	4.50	2.81	4.11	7.31	31.63	38.44
BA	0.70	4.60	2.70	7.82	1.80	0.50	0.50	4.70	2.32	2.82	7.02	17.73	33.05
Bw	0.50	5.00	0.10	3.91	1.70	1.80	0.10	4.60	3.51	3.61	8.11	2.77	43.28
P4 - *Chernossolo Argilúvico Órtico saprolítico - MTo* (Typic Argiustoll - TAoll)													
A	1.90	6.10	1.02	89.93	21.20	7.70	0.04	5.20	29.13	29.17	34.33	0.14	84.85
BA	0.70	6.40	5.62	58.65	21.20	6.30	0.04	3.70	27.65	27.69	31.35	0.14	88.20
Bt	0.20	6.40	0.34	58.65	20.90	7.20	0.04	3.30	28.25	28.29	31.55	0.14	89.54
BC	0.10	6.80	0.43	58.65	23.30	6.40	0.06	2.70	29.85	29.91	32.55	0.20	91.71
CR	0.10	6.70	0.21	19.55	20.80	8.80	0.28	2.40	29.65	29.93	32.05	0.94	92.51

OM: organic matter (Walkley-Black method); P and K: extractor Mehlich-1; Ca^{2+}, Mg^{2+}, Al^{3+}: extractor 1 mol L^{-1} KCl; H+Al: potential acidity, extractor 0.5 mol L^{-1} calcium acetate; SB: sum of bases; t: effective cation exchange capacity (SB+Al^{3+}); CEC: cation exchange capacity at pH7; m: aluminum saturation; V: base saturation.

Table 3. Chemical composition, expressed in the oxide basis of the element, as determined through sulfuric attack and Ki and Kr indices for samples from the Southern Espinhaço Mountain Chain and Upper Jequitinhonha Valley

Soil[(1)]	Horizon	SiO_2	Al_2O_3	Fe_2O_3	TiO_2	MnO	Ki[(2)]	Kr[(3)]
		%						
P1 - RKox	Bn_1	19.4	22.03	17.52	26.09	0.04	1.49	0.99
P2 - RHox	Bw	14.7	20.14	22.51	37.04	0.12	1.24	0.72
P3 - THox	Bw	26.4	35.24	10.06	14.64	0.03	1.27	1.07
P4 - TAoll	Bt	23.0	13.16	12.26	1.69	0.15	2.97	1.85

[(1)] P1- *Nitossolo Vermelho Distroférrico típico - NVdf* (Rhodic Kandiustox - RKox), P2 - *Latossolo Vermelho Distroférrico típico - LVdf* (Rhodic Haplustox - RHox), P3 - *Latossolo Vermelho Distrófico típico - LVdf* (Typic Haplustox - Thox), P4 - *Chernossolo Argilúvico Órtico saprolítico - MTo* (Typic Argiustoll - TAoll). [(2)] Ki = [(%SiO_2 × 1.697)/%Al_2O_3]. [(3)] Kr: (%SiO_2 × 1.697)/[(%Al_2O_3) + (%Fe_2O_3 × 0.64)].

pedogenetic processes of accumulation and removal (Kämpf and Curi, 2000). Thus, the TAoll, a less weathered soil, may be a residual accumulation of these oxides.

The RHox and TAoll had higher MnO levels than the other soils because they are derived from basic rocks. Higher TiO_2 contents were found in the RKox and RHox (Table 3) and can be associated with minerals inherited from igneous rocks (Kämpf and Schwertmann, 1982), such as anatase, which is found in the clay and sand fractions (Costa, 2014) .

The Ki index was high only for the TAoll (Table 3). This index provides an estimate of the degree of weathering of tropical and subtropical soils and the relationship of kaolinite and gibbsite in soils (Oliveira, 2001). Mello et al. (1995) suggest the occurrence of 2:1 clay when Ki >2.2. In fact, mineralogical analysis of the clay fraction of the Bt horizon in the TAoll revealed the occurrence of hydroxy-interlayered vermiculite (Costa, 2014). The Ki index allowed the framework for other profiles in the Oxisols class (Ki <2.2), except for the RKox, which has a kandic B horizon. The high weathering stage of iron-free clay mineralogy of Oxisols, kaolinitic and gibbsitic (Costa, 2014), are shown by intense desilicatization, which is typical of ferralitic weathering (Rodrigues and Klamt, 1978; Breemen and Buurman, 2002). Similar results were found by Ferreira et al. (2010) and Bispo et al. (2011a, b) for Oxisols in UVJ toposequences.

The Kr index is appropriate for indicating the degree of alteration that reflects the evolution of minerals in the soil (Carvalho, 1956). In the RKox and TAoll, soils that are less weathered and obtained from green schist, the presence of gibbsite was not detected in the clay fraction (Costa, 2014). Ferreira et al. (2010) and Bispo et al. (2011a, b) found similar results for Oxisols of the UVJ plateaus.

The TAoll contained higher levels of Fe_o, lower levels of Fe_d, and the highest Fe_o/Fe_d ratio (Table 4) because, despite having more than 12 % Fe_2O_3 (Table 3), part of the iron oxides are of low crystallinity (about 14 %), typical of less weathered soil (Kämpf and Curi, 2000). Soils with higher Fe_d levels and lower Fe_o/Fe_d ratios (Table 4) were those with a ferric character (RHox and RKox) and high total concentrations of iron oxides (Table 3). According to Kämpf and Curi (2000), elevated Fe_d levels indicate the presence of iron oxides of high crystallinity.

The TAoll, the least weathered soil, contained the lowest levels of Al_d and the highest Al_o/Al_d ratios (Table 3), indicating the predominance of more amorphous forms of Al (Andrade et al., 1997). Soils with ferric character (RHox and RKox) had intermediate levels of Al_o, Al_d (Table 4), and Al_2O_3 (Table 3), but their Al_o/Al_d ratios were low (Table 4), indicating the predominance of Al crystalline forms (Alleoni and Camargo, 1994).

Table 4. Iron, aluminum, and manganese contents for the ammonium oxalate (OAA) and dithionite-citrate-bicarbonate (DCB) extracts, and Fe_o/Fe_d and Al_o/Al_d ratios for samples from soils of the Southern Espinhaço Mountain Chain and Upper Jequitinhonha Valley

Soil[(1)]	Horizon	OAA		DCB		Fe_o/Fe_d	Al_o/Al_d
		Al	Fe	Al	Fe		
		g kg^{-1}					
P1 - RKox	Bn1	1.83	1.89	8.16	50.37	0.04	0.22
P2 - RHox	Bw	1.87	3.50	10.90	70.14	0.05	0.17
P3 - THox	Bw	3.10	1.40	7.86	39.45	0.04	0.39
P4 - TAoll	Bt	2.40	4.46	4.30	31.22	0.14	0.56

[(1)] P1- *Nitossolo Vermelho Distroférrico típico - NVdf* (Rhodic Kandiustox - RKox), P2 - *Latossolo Vermelho Distroférrico típico - LVdf* (Rhodic Haplustox - RHox), P3 - *Latossolo Vermelho Distrófico típico - LVdf* (Typic Haplustox - Thox), P4 - *Chernossolo Argilúvico Órtico saprolítico - MTo* (Typic Argiustoll - TAoll).

The Fe_d and Al_d levels increase in the following sequence in the soil from basic rocks: TAoll > RKox > RHox (Table 4), thereby demonstrating the ferralitization process that is caused by increased weathering.

Kaolinite (Ka) was identified by XRD reflections related to basal spacings of 0.724, 0.357, and 0.45 nm, which collapsed after heating at 550 °C (Figure 2). Anatase (An) is identified by the reflection at 0.351 nm, which is clearer after heating at 550 °C, and by the oxide concentrate sample. The hydroxy-interlayered vermiculite (HIV) found in the TAoll was identified by diffraction peaks at 0.682, 0.376, and 0.40 nm, which showed no displacement after treatment with glycerol and collapsed after heating at 550 °C (Figure 2). Reflections on the gibbsite (Gb) in the THox are located at 0.424, 0.541, 0.471, and 0.437 nm. In the RHox, they are located at 0.588 and 0.612 nm. The mineralogical composition is consistent with the results of chemical analyses (Tables 3 and 4).

The Ka occurs in all soils, Gb in Latosols, and An in Oxisols (Figure 2). The An is titanium oxide, frequently observed in soil materials from regions with predominance of Oxisols (Curi and Franzmeier, 1987; Ferreira et al., 2010; Bispo et al, 2011a,b). The hydroxy-interlayered vermiculite (HIV) was identified in the TAoll (Figure 2). It is a common mineral in less weathered soils (Clemente et al., 2000).

Oxisols are essentially composed of Ka and Gb, typical of soils formed by intense weathering under good drainage conditions (Curi and Franzmeier, 1987). These results are supported by lower Ki values (Table 3) and low Fe_o/Fe_d ratios (Table 4).

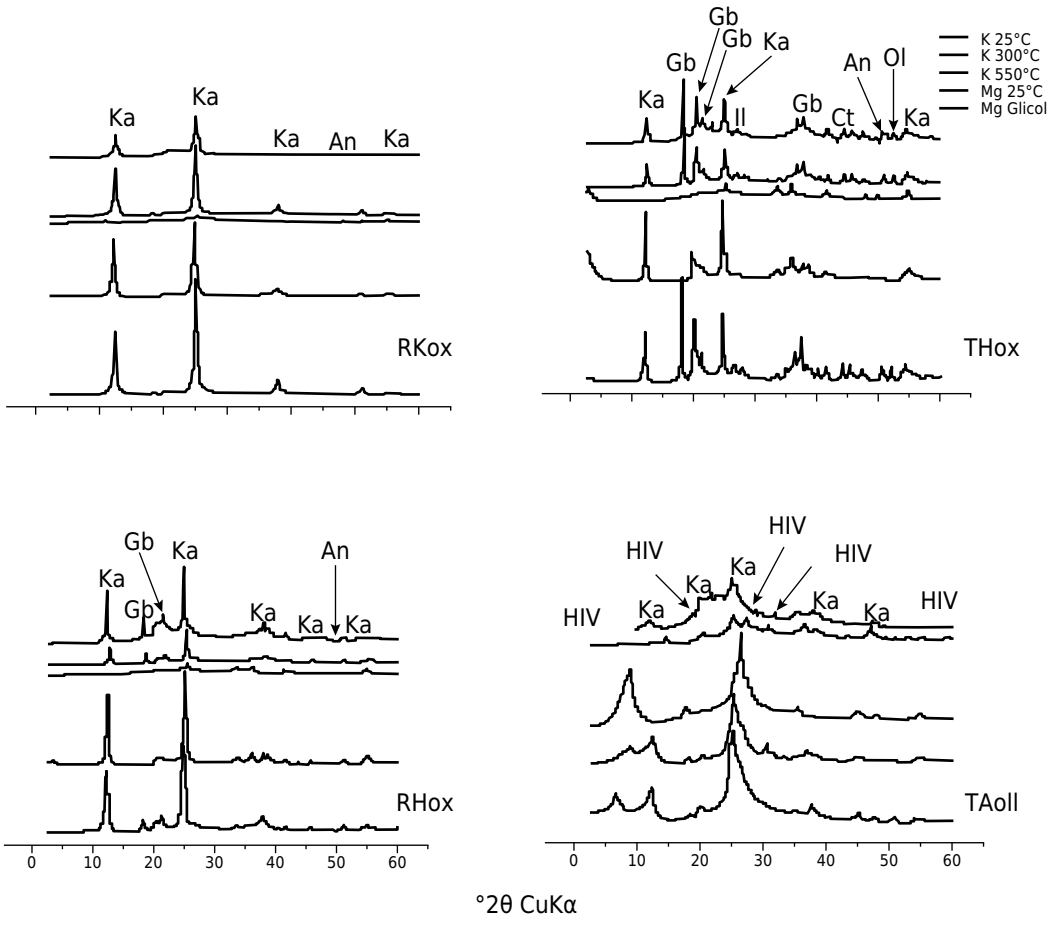

Figure 2. X ray diffraction patterns for clay fractions from the soil diagnostic horizons. Ka: kaolinite; Gb: gibbsite; Ct: chlorite; An: anatase; and HIV: hydroxy-interlayered vermiculite.

The mineralogy of the TAoll, RKox, and RHox, respectively, Ka + HIV, Ka and Ka + Gb (Figure 2) also show the progress of desilicatization and ferralitization processes with the intensification of weathering.

The mineralogical composition of the clay fraction of the diagnostic horizons, obtained by differential X ray diffraction (Figure 3), consists mainly of goethite (Gt), with weak reflections of hematite (Hm) and strong reflections between magnetite (Mt) and maghemite (Mh).The strong reflection are indicative of the greater crystallinity of these minerals (Troeh and Thompson, 2007). For the RKox, THox, RHox, and TAoll, weak reflections, indicative of the presence of feldspar (Fd), were observed between 0.37 and 0.35 nm, between 0.35 and 0.40 nm, at 0.35 nm, and between 0.35 and 0.32 nm, respectively (Brown and Brindley, 1980). Little evidence of the occurrence of calcium feldspar (Fc) was found in the reflection at 0.30 nm in the RKox. This property is characteristic of the weathering of green schist (Freitas and Argentin, 2010). Ferrihydrite traces (Fr) were found in the THox at 0.25 nm. Traces of olivine (Ol) were detected in the RKox between 0.25 and 0.37 nm, in the THox at 0.37 nm, and in the TAoll at 0.25 nm. An was found in all the soils. A diffraction peak at 0.37 nm was found in the RKox and THox, at 0.32 nm in the RHox, and at 0.42 nm in the TAoll. Traces of mica (Mi) in Oxisols can be inferred by the reflection at 0.25 nm. Amphibole (Af) was found in the THox through the reflection at 0.30 nm and in the RHox by reflection at 0.25 nm. Biotite (Bt) and chlorite (Ct) were found in the THox, with a significant peak at 0.35 nm. Other minerals found in the RHox and associated with similar reflections were corundum (Ci) and An. Potassium feldspar (Fk) was found in the TAoll material through the reflection at 0.25 nm. Talc (Tc) was found only for the TAoll, through the reflection at 0.28 nm. The minerals identified by X ray differential diffraction (Figure 3) reflect the source material and the weathering stage of the soils.

The mineralogical composition of the sand fraction of the diagnostic horizons of the soils, obtained by X ray diffraction (Figure 4), is primarily quartz (Qz) and Mt. Weak reflections were observed, indicative of the occurrence of Fd (Sampaio et al., 2006), for the RKox, THox, RHox, and TAoll from 0.37 to 0.35 nm, from 0.35 to 0.40 nm, at 0.35 nm, and from 0.35 to 0.32 nm, respectively. For the TAoll, a strong reflection of Fc was obtained at

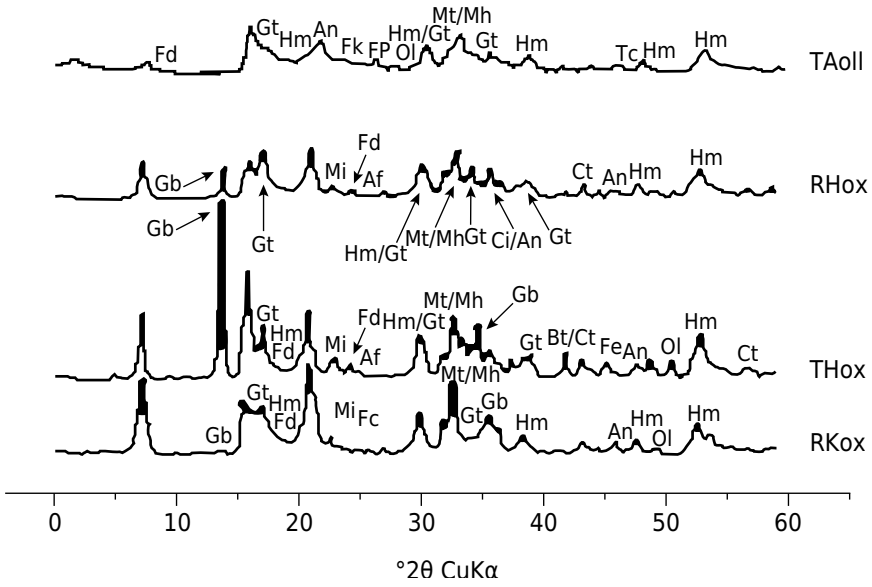

Figure 3. X ray diffraction patterns for the clay fraction from samples of the diagnostic horizons. Gb: gibbsite; Gt: goethite; Fd: feldspar; Hm: hematite; Hm/Gt: hematite/goethite; Mt/Mh: magnetite/maghemite; Fr: ferrihydrite; Fc: calcium feldspar; Ol: olivine; An: anatase; Mi: mica; Af: amphibole; Bt/Ct: biotite/chlorite; Ci/An: corundum/anatase; Ct: chlorite; Fk: potassium feldspar; and Tc: talc.

0.25 nm. The Fc constituent is from green schist (Brown and Brindley, 1980). According to Queiroga (2006), Af is a constituent mineral of gabbros and has been detected in the RHox in a strong single reflection at 0.282 nm.

Fe^{3+} was found in all the soils. Magnetite, Hm, and Fe^{2+} were found in the TAoll; for the RKox and THox, Mh and Hm were detected; and Mh and Fe^{2+} were identified in the RHox (Table 5).

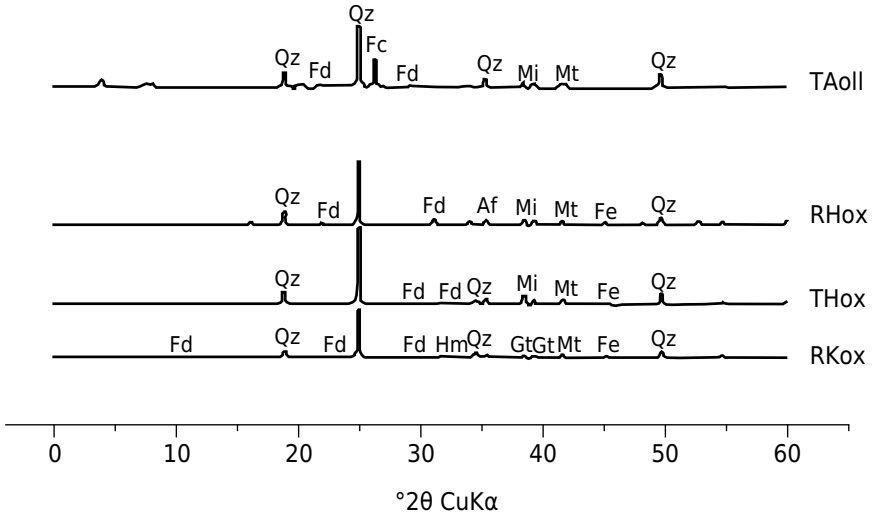

Figure 4. X ray diffraction patterns for the sandy fraction from the diagnostic soil horizons. Fd: feldspar; Fc: calcium feldspar; Qz: quartz; Af: amphibole; Mi: mica; Hm: hematite; and Mt: magnetite.

Table 5. ^{57}Fe hyperfine spectral parameters at room temperature (~298 K) for samples from soils of the Southern Espinhaço Mountain Chain and Upper Jequitinhonha Valley

Oxide	Δ/mms^{-1}	2ε$_Q$ or Δ/mms^{-1}	B$_{hf}$/T	RA/%
P1- *Nitossolo Vermelho Distroférrico típico - NVdf* (Rhodic Kandiustox - RKox)				
Hm	0.261(1)	-0.174(2)	50.11(2)	56.50
Mh	0.245(3)	0*	46.64(3)	19.50
Fe^{3+}	0.249(2)	0.570(3)		24.00
P2 - *Latossolo Vermelho Distróférrico típic - LVdf* (Rhodic Haplustox - RHox)				
Hm	0.270(3)	-0.200(2)	49.56(2)	25.40
Mh	0.212(2)	0*	45.90(1)	20.30
Fe^{3+}	0.244(3)	0.549(3)		48.30
Fe^{2+}	1.020(2)	0.622(2)		6.00
P3 - *Latossolo Vermelho Distrófico típico- LVd* (Typic Haplustox - THox)				
Hm	0.266(1)	-0.180(2)	50.25(**)	45.60
Mh	0.213(3)	0*	47.10(4)	31.20
Fe^{3+}	0.251(2)	0.560(3)		23.20
P4 - *Chernossolo Argilúvico Órtico saprolítico – MTo* (Typic Argiustoll – Taoll)				
[Mt]	0.250*	0*	47.20(3)	8.40
{Mt}	0.550*	0*	45.00(5)	5.05
Fe^{3+}	0.235(3)	0.617(4)		81.76
Fe^{2+}	1.740(3)	1.140(6)		4.80

δ: isomeric shift relative to αFe; 2εQ: quadrupole shift; Δ: quadrupole splitting, and AR: relative subspectral area. Hm: hematite; Mh: maghemite; [Mt]: Fe^{3+} in the magnetite tetrahedral site; {Mt}: $Fe^{3+/2+}$ in the magnetite octahedral site; (*): fixed parameter. The numbers in parentheses are uncertainties over the last significant digit of the corresponding values, estimated as standard deviation as output from the non-linear least squares method, according to the computer algorithm used for numerical fitting of the Mössbauer spectra to Lorentzian functions of the resonance lines.

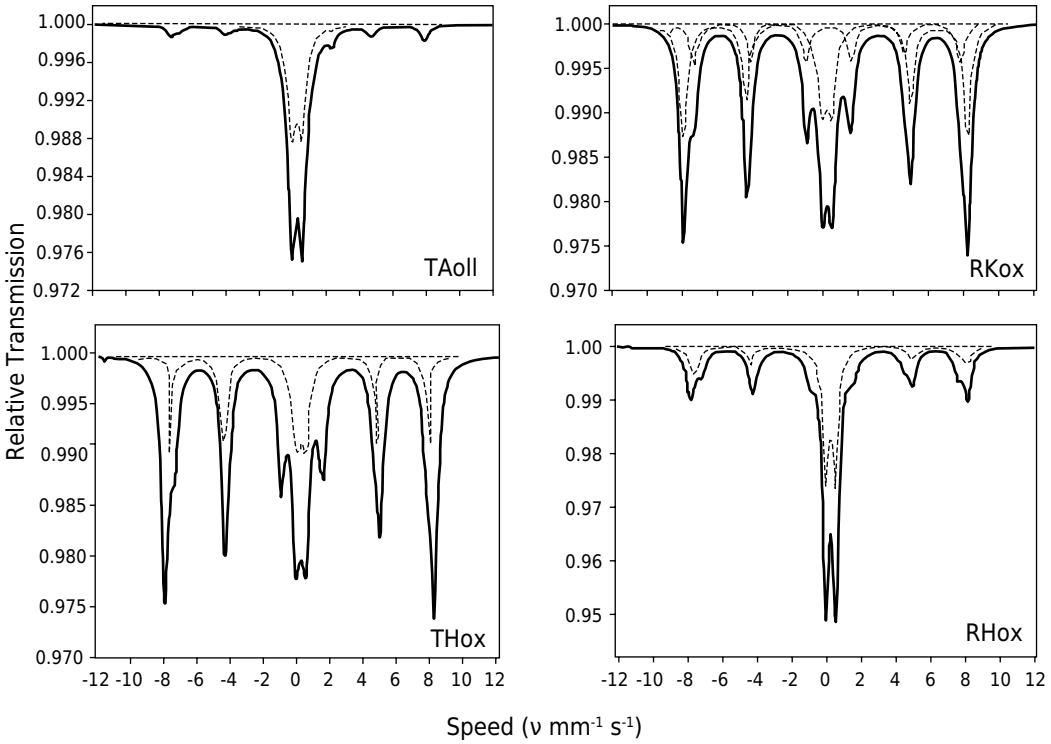

Figure 5. ^{57}Fe Mössbauer spectra at ~298 K for samples from the diagnostic soil horizons.

Safe and detailed analysis of the Mössbauer spectra (Figure 5) obtained without an applied magnetic field cannot be direct. Some semiquantitative information, however, was obtained from general characteristics of the spectra. For the RKox and THox samples, patterns of spectral contributions of magnetically ordered species and a central doublet were similar (Figure 5), but the proportions of the relative subspectrum areas (RA) were different (Table 5).

For the RHox, a sextet of Mh and two doublets were found, an Fe^{3+} and another of Fe^{2+} (Figure 5). The Fe^{2+} doublet is attributable to ilmenite (FeTiO3).

For the sample of the TAoll, the spectrum was completely dominated by an intense central doublet of Fe^{3+}. A doublet of Fe^{2+} was also observed (Figure 5). However, because of the low amount of resonance, a definitive adjustment for an Fe^{2+} paramagnetic subspectrum, most likely the aluminosilicate structure, was not observed. It is also possible to assign subspectra relating to tetrahedral [Fe^{3+}] and octahedral [$Fe^{3+}/^{2+}$] relating to magnetite, although the intensities of the corresponding resonance lines were only incipient.

The images obtained by scanning electron microscopy of sand, silt, clay, and magnetic fractions are in figure 6, in which the highlighted fields had the contents of major elements quantified by dispersive energy spectroscopy.

All the soils have only Si in the sand fraction, except for the RKox, which is predominantly Fe and Ti (Table 6); Ti also predominated in sulfuric attack on the fine earth fraction of the RKox (Table 3). Hematite and magnetite were identified in the sand fraction of the RKox (Figure 4).

All the soils contained Si and Al in the silt fraction. The soils derived from basic rocks (RKox, RHox, and TAoll) contained Fe in the silt fraction, which strongly predominates in those with a ferric character (Table 6). The TAoll, less weathered, has Mg and Na in this fraction (Table 6).

In the RKox clay fraction, the content of major elements showed the following descending order: Si ~ Al > Fe > Ti (Table 6). These results are in agreement with those obtained from sulfuric attack (Ti > Al ~ Si > Fe; Table 3), except for Ti, which predominates in the

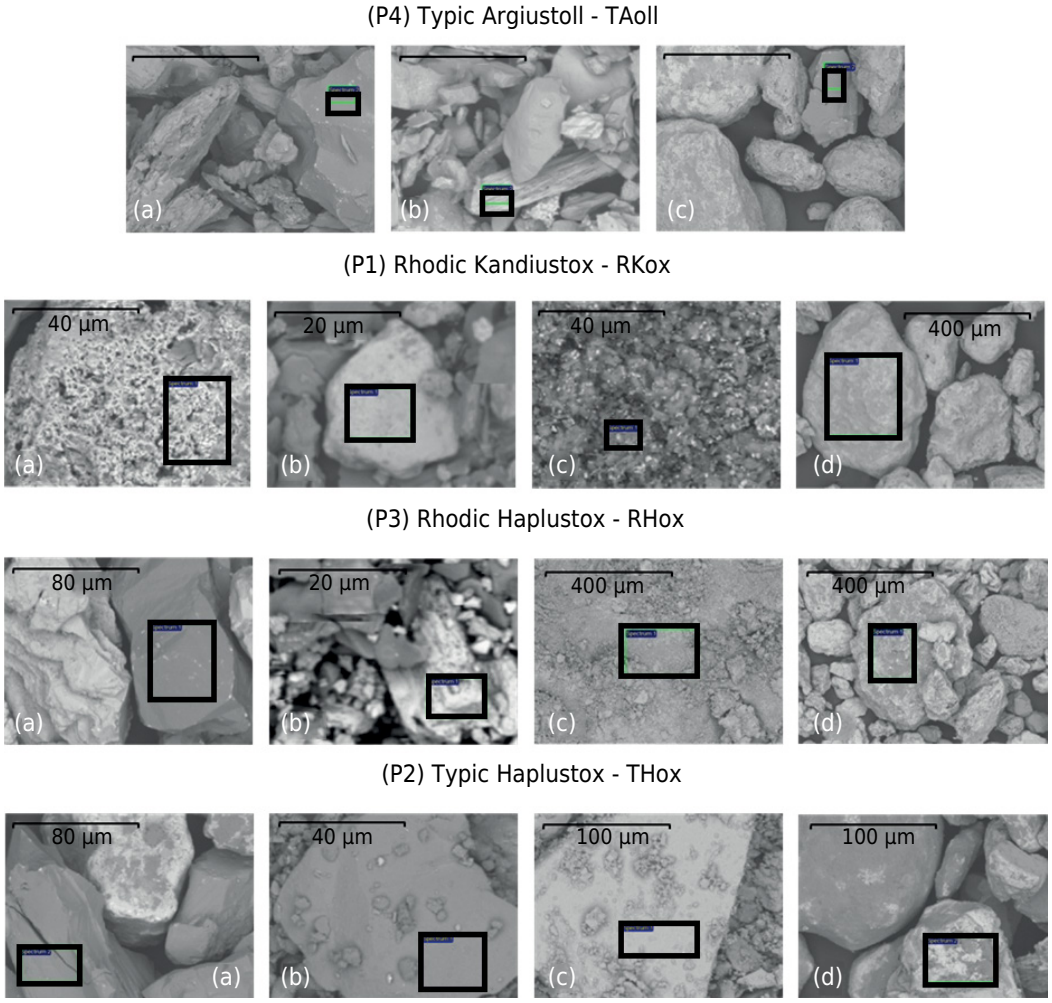

Figure 6. Scanning electron microscopy for the (a) sand, (b) silt, and (c) clay fraction and (d) magnetic extract from the diagnostic horizons of the soils. The fields marked as square labels refer to probing points by energy dispersive spectroscopy.

sand fraction (Table 6). The results are also in agreement with their mineralogy because kaolinite, anatase, hematite, goethite, and maghemite were identified (Figures 2 and 3).

The content of the major elements in the THox clay fraction was observed in the following descending order: Al > Si > Fe (Table 6). These results were also obtained from sulfuric attack (Al > Si > Fe; Table 3) and are supported by clay mineralogy, in which kaolinite, gibbsite, hematite, goethite, ferrihydrite, and maghemite were identified (Figures 2 and 3).

For the RHox clay, the following sequence of the major elements was found: Al > Fe > Si (Table 6). The same result was obtained by sulfuric attack [Al > Fe > Si (Table 3)], and this was supported by their mineralogy because kaolinite, gibbsite, hematite, and maghemite were identified (Figures 2 and 3).

Siliceous predominated in the clay fraction of the TAoll, followed by Fe, Al, and Mg (Table 6). These results are consistent with those obtained by sulfuric attack [Si > Al ~ Fe (Table 3)] and with clay mineralogy, formed by kaolinite, hydroxy-interlayered vermiculite, goethite, hematite, and maghemite (Figures 2 and 3).

In less weathered soils (TAoll and RKox), Si predominated; in the most weathered (THox and RHox), Al predominated in the clay fraction (Table 6). The Fe content in the clay fraction ranged from 8.9 to 4.4 % and showed the following decreasing order in the diagnostic horizons: TAoll > ~THox > RKox.

Table 6. Major elemental chemical composition for the sand, silt, and clay fractions from diagnostic horizons of the soils from the Southern Espinhaço Mountain Chain and Upper Jequitinhonha Valley, as obtained by dispersive energy spectroscopy

Fraction	O	Si	Al	Fe	Ti	Mg	Na
	%						
P1- *Nitossolo Vermelho Distroférrico típico - NVdf* (Rhodic Kandiustox - RKox)							
Sand	71.2	4.7	3.3	10.0	10.8	-	-
Silt	67.2	4.0	3.1	28.7	-	-	-
Clay	73.0	10.6	10.4	4.4	1.2	-	0.4
Magnetic extract	64.1	5.8	4.2	25.9	-	-	-
P2 - *Latossolo Vermelho Distróférrico típico - LVdf* (Rhodic Haplustox - RHox)							
Sand	68.8	31.2	-	-	-	-	-
Silt	64.7	1.3	4.8	29.2	-	-	-
Clay	74.6	7.2	10.2	8.0	-	-	-
Magnetic extract	65.6	4.4	9.8	21.2	-	-	-
P3 - *Latossolo Vermelho Distrófico típico - LVd* (Typic Haplustox - THox)							
Sand	56.1	46.9	-	-	-	-	-
Silt	68.1	30.4	1.5	-	-	-	-
Clay	65.0	8.3	20.5	5.6	-	-	0.6
Magnetic extract	62.0	6.4	8.6	21.7	-	-	1.3
P4 - *Chernossolo Argilúvico Órtico saprolítico - MTo* (Typic Argiustoll - TAoll)							
Sand	66.7	33.3	-	-	-	-	-
Silt	64.8	20.8	1.9	5.7	-	5.7	1.1
Clay	71.4	11.0	7.5	8.9	-	1.2	-

Large predominance of Fe in the magnetic fraction and the occurrence of Al and Si were detected. In the THox and RHox, the Al content exceeded Si, and the opposite occurred in the RKox (Table 6).

It should be recognized that the chemical composition data obtained by dispersive energy spectroscopy, an analytical technique of site probing (areas marked in figure 6) in the sample space, can be discrepant from the analysis of the total sample, such as sulfuric attack by opening. The chemical compositions given by the two methods should therefore consider the methodological characteristics in each case.

CONCLUSIONS

Maghemite (γFe_2O_3) was found in all the soils, and magnetite (Fe_3O_4) was identified only in the TAoll.

There is evidence that the occurrence of magnetic minerals is related to the source material.

The soils derived from basic rocks have magnetic iron oxides dependent on the weathering stage.

The desilicatization and ferralitization processes were demonstrated in a decreasing sequence of weathering in soil originating from basic rocks: TAoll > RKox > RHox.

ACKNOWLEDGMENTS

We thank the Universidade Federal dos Vales do Jequitinhonha e Mucuri (UFVJM) for institutional support, the CNPq (Grant No. 305755-2013-7), Fapemig (Grant No. CEX - PPM-00412-15) and Capes (PNPD 2606/2011, process No. 2338007759/2011-52) for

financial support and scholarships. JDF thanks CAPES for the PVNS grant in effect at the Federal University of Vales do Jequitinhonha and Mucuri (Diamantina, MG).The authors are indebted to professor David Lee Nelson (UFVJM) for kindly reading the manuscript and for all the suggestions presented, particularly those concerning the English language.

REFERENCES

Alleoni LRF, Camargo OA. Potencial elétrico superficial e carga elétrica líquida de Latossolos ácricos. Rev Bras Cienc Solo. 1994;18:181-5.

Almeida-Abreu PA, Renger FE. Serra do Espinhaço Meridional: um Orógeno de Colisão do Mesoproterozóico. Geonomos. 2002,32:1-13.

Andrade H, Schaefer CE, Demattê JLI, Andrade FV. Pedogeomorfologia e micropedologia de uma sequência Latossolo-Areia Quartzoza Hidromórfica sobre rochas cristalinas do estado do Amazonas. Geonomos. 1997;5:55-66.

Bispo FHA, Silva AC, Torrado PV. Highlands of the upper Jequitinhonha Valley, Brazil. I - Characterization and classification. Rev Bras Cienc Solo. 2011a;35:1069-80. https://doi.org/10.1590/S0100-06832011000400001

Bispo FHA, Silva AC, Torrado PV. Highlands of the upper Jequitinhonha Valley, Brazil. II – Mineralogy, micromorphology and landscape evolution. Rev Bras Cienc Solo. 2011b;35:1081-91. https://doi.org/10.1590/S0100-06832011000400002

Brasil. Ministério do Planejamento e Orçamento. Fundação Instituto Brasileiro de Geografia e Estatística - IBGE. Diagnóstico Ambiental da Bacia do Rio Jequitinhonha. Salvador: IBGE/Diretoria de Geociências; 1997.

Breemen NV, Buurman P. Soil formation. 2nd ed. Dordrecht: Kluwer; 2002.

Brown G, Brindley GW. X-ray diffraction procedures for clay mineral identification. In: Brindley GW, Brown G, editors. Crystal structures of clay minerals and their X-ray identification. London: Mineralogical Society; 1980.

Carvalho GBCT. Método rápido de determinação das relações ki e kr em solos. Rio de Janeiro: Instituto de Química Agrícola; 1956. (Boletim, 48).

Chaves LHG, Vasconcelos ACF. Alterações de atributos químicos do solo e do crescimento de plantas de milho pela aplicação de xisto. Rev Bras Eng Agríc Amb. 2006;10:84-8. https://doi.org/10.1590/S1415-43662006000100013

Chula AMD. Caracterização geológica e geoquímica dos metamagmatitos e metassedimentos da Região de Planalto de Minas, Município de Diamantina, MG. Rev Bras Geocienc. 1998;28:246-52.

Claessen MEC, organizador. Manual de métodos de análise de solo. 2a ed. Rio de Janeiro: Centro Nacional de Pesquisa de Solos; 1997.

Clemente CA, Demattê JAM, Mafra AL, Bentivenha SRP. Reflectância espectral e mineralogia de materiais formados sobre diabásio. Sci Agríc. 2000;57:159-68. https://doi.org/10.1590/S0103-90162000000100026

Costa RV. Características mineralógicas e químico-estruturais de óxidos de ferro e potencial agrícola de solos magnéticos da Serra do Espinhaço Meridional e do Alto Vale do Jequitinhonha [dissertação]. Diamantina: Universidade Federal dos Vales do Jequitinhonha e Mucuri; 2014.

Cunha P, Marques Junior J, Curi N, Pereira GT, Lepsch IF. Superfícies geomórficas e atributos de Latossolos em uma sequencia Arenítico-Basáltica da região de Jaboticabal (SP). Rev Bras Cienc Solo. 2005;29:1-90. https://doi.org/10.1590/S0100-06832005000100009

Curi N, Franzmeier DP. Effect of parent rocks on chemical and mineralogical properties of some Oxisols in Brazil. Soil Sci Soc Am J. 1987;51:153-8. https://doi.org/10.2136/sssaj1987.03615995005100010033x

Fabris JD, Coey JMD, Mussel WN. Magnetic soils from mafic lithodomains in Brazil. Hyper Interac. 1998;113:249-58.

Fabris JD, Coey JMD. Espectroscopia Mössbauer do ^{57}Fe e medidas magnéticas na análise de geomateriais. Tópicos Cienc Solo. 2002;2:47-102.

Fabris JD, Viana JHM, Schaefer CEGR, Wypych F, Stucki JW. Métodos físicos de análises em mineralogia do solo. In: Melo VF, Alleoni LRF, editores. Química e mineralogia do solo; Conceitos básicos. Viçosa, MG: Sociedade Brasileira de Ciência do Solo; 2009.

Ferreira SAD, Santana DP, Fabris JD, Curi N, Nunes Filho E, Coey JMD. Relações entre magnetização, elementos traços e litologia de duas sequências de solos do estado de Minas Gerais. Rev Bras Cienc Solo. 1994;18:167-74.

Ferreira CA, Silva AC, Torrado PV, Rocha WW. Genesis and classification of Oxisols in a highland toposequence of the Upper Jequitinhonha Valley, MG. Rev Bras Cienc Solo. 2010;34:195-210. https://doi.org/10.1590/S0100-06832010000100020

Figueiredo MA, Fabris JD, Varajao AFDC, Couceiro PRC, Loutfi IS, Azevedo IS, Garg VK. Óxidos de ferro de solos formados sobre gnaisse do Complexo Bação, Quadrilátero Ferrífero, Minas Gerais. Pesq Agropec Bras. 2006;41:313-21. https://doi.org/10.1590/S0100-204X2006000200017

Freitas J, Argentin PM. K-Feldspatos, GE300/A - Mineralogia. Campinas: Unicamp; 2010.

Gradim RJ, Alkmim FF, Pedrosa-Soares AC, Babinski ME, Noce CM. Xistos Verdes do Alto Araçuaí, Minas Gerais: Vulcanismo Básico do Rifte Neoproterozóico Macaúbas. Rev Bras Geocienc. 2005;35:59-69. https://doi.org/10.5327/rbg.v35i4.1207

Inda Junior AV, Kämpf N. Avaliação de procedimentos de extração dos óxidos de ferro pedogênicos com ditionito-citrato-bicarbonato de sódio. Rev Bras Cienc Solo. 2003;27:1139-47. https://doi.org/10.1590/S0100-06832003000600018

Inda Junior AV, Bayer C, Conceição PC, Boeni M, Salton JC, Tonin AT. Variáveis relacionadas à estabilidade de complexos organo-minerais em solos tropicais e subtropicais brasileiros. Cienc Rural. 2007;37:1301-7. https://doi.org/10.1590/S0103-84782007000500013

Jackson ML. Soil chemical analysis - Advanced course. Madison: Prentice-Hall; 1969.

Kämpf N, Schwertmann U. The 5 M-NaOH concentration treatment for iron oxides in soil. Clays Clay Miner. 1982;30:401-8.

Kämpf N, Curi N. Óxidos de ferro: Indicadores de ambientes pedogênicos e geoquímicos. Tópicos Cienc Solo. 2000;1:107-38.

Leal JR. Adsorção de fósforo em Latossolos sob cerrado [dissertação]. Itaguaí: Universidade Federal Rural do Rio de Janeiro; 1971.

Mckeague JA, Day JH. Dithionite and oxalate-extractable Fe and Al as aids in differentiating various classes of soils. Can J Sci. 1966;46:13-22.

Mehra OP, Jackson ML. Iron oxide removal from soils and clay by a dithionite-citrate system buffered with sodium bicarbonate. Clays Clay Miner. 1960;7:317-27.

Mello VF, Costa LM, Barros NF, Fontes MPF, Novais RF. Reserva mineral e caracterização mineralógica de alguns solos do Rio Grande do Sul. Rev Bras Cienc Solo. 1995;19:159-64.

Minas Gerais. Secretaria de Planejamento. Indicadores socio-econômicos: 1950-1980. Belo Horizonte: Seplan/Superintendência de Estatística e Informações; 1983.

Moore DM, Reynolds RC. X-ray diffraction and identification and analysis of clay minerals. Oxford: Oxford University Press; 1989.

Muggler CC, van Loef JJ, Buurman P, van Doesburg JDJ. Mineralogical and (sub)microscopic aspects of iron oxides in polygenetic Oxisols from Minas Gerais, Brazil. Geoderma. 2001;100:147-71. https://doi.org/10.1016/S0016-7061(00)00084-7

Norrish K, Taylor M. The isomorphous replacement of iron by aluminium in soil goethites. J Soil Sci. 1961;12:294-306.

Novais RF, Neves JCL, Barros NF. Aspectos físicos-químicos envolvidos na fixação de fósforo no solo. In: Anais do 5º Encontro Nacional de Rocha Fosfática; 1991. São Paulo: 1991. p.133-77.

Novais RF, Smyth TJ, Nunes FN. Fósforo. In: Novais RF, Alvarez V VH, Barros NF, Fontes RLF, Cantarutti RB, Neves JCL, editores. Fertilidade do solo. Viçosa, MG: Sociedade Brasileira de Ciência do Solo; 2007.

Oliveira JB. Pedologia aplicada. Jaboticabal: Funeb; 2001.

Popp JH. Geologia geral. 6a ed. Rio de Janeiro: LTC; 1998.

Portal da Cidadania. Brasília, DF: Instituto Nacional da Colonização e Reforma Agrária; 2011 [accessed on: 15 Oct. 2012]. Available at: http://www.territoriosdacidadania.gov.br.

Queiroga GN. A seção sedimentar sulfetada do ofiolito de Ribeirão da Folha e seu potencial metalogenético, Orógeno Araçuaí, MG [dissertação]. Belo Horizonte: Universidade Federal de Minas Gerais; 2006.

Resende M, Coey JMD, Allan J. The magnetic soils of Brazil. Earth Planet Sci Lett. 1986;78:322-6.

Resende M, Curi N, Santana DP. Pedologia e fertilidade do solo. Interações e aplicações. Brasília, DF: Ministério da Educação; Piracicaba: Esalq/Potafos; 1988.

Resende M, Curi N, Rezende SB, Corrêa GF. Pedologia: base para distinção de ambientes. 5a ed. Lavras: Universidade Federal de Lavras; 2007.

Rodrigues TE, Klamt E. Mineralogia e gênese de uma sequência de solos do Distrito Federal. Rev Bras Cienc Solo. 1978;2:132-9.

Sampaio VG, Pinheiro BCA, Holanda JNF. Granulação e caracterização de uma massa cerâmica para porcelanato. In: Anais do 17º Congresso Brasileiro de Engenharia e Ciência dos Materiais; 2006; Foz do Iguaçu. Foz do Iguaçu: 2006.

Santos HG, Jacomine PKT, Anjos LHC, Oliveira VA, Oliveira JB, Coelho MR, Lumbreras JF, Cunha TJF. Sistema brasileiro de classificação de solos. 3a ed. Rio de Janeiro: Embrapa Solos; 2013.

Santos RD, Lemos RC, Santos HG, Ker JC, Anjos LHC. Manual de descrição e coleta de solo no campo. 5a ed. Viçosa, MG: Sociedade Brasileira de Ciência do Solo; 2005.

Schwertmann U, Taylor RM. Iron oxides. In: Dixon JB, Weed SB, editors. Minerals in soil environments. Madison: Soil Science Society of America; 1977.

Schwertmann U. Some properties of soil and synthetic iron oxides. In: Stucki JW, Goodman BA, Schwertmann U, editors. Iron in soils and clay minerals. Dordrecht: D. Reidel; 1989.

Silva AC, Pedreira LCVSF, Almeida Abreu PA. Serra do Espinhaço Meridional: paisagens e ambientes. Belo Horizonte: O Lutador; 2005.

Soil Survey Staff. Keys to soil taxonomy. 11th ed. Washington, DC: United States Department of Agriculture, Natural Resources Conservation Service; 2010.

Theisen AA, Harward ME. A paste method for preparation of slides for clay mineral identification by x-ray diffraction. Soil Sci Soc Am Proc. 1962;26:90-1.

Troeh FR, Thompson LM. Solos e fertilidade do solo. 6a ed. São Paulo: Organização Andrei; 2007.

Vahl LC. Fertilidade de solos de várzea. In: Gomes AS, Pauletto EA, editores. Manejo de solo e da água em áreas de várzea. Pelotas: Embrapa Clima Temperado; 1999.

Vilhena CF, Gontijo M, Viveiros NCS. Estudo técnico para a extensão dos perímetros do Parque Estadual do Rio Preto e do Parque Estadual do Pico do Itambé na Região do Alto Jequitinhonha. Belo Horizonte: Instituto Estadual de Florestas; 2010.